Frequency comb induced radiative force on cold rubidium atoms

G. Kregar,[1] N. Šantić,[2, 1] D. Aumiler,[1] H. Buljan,[2] and T. Ban[1]

[1]*Institute of Physics, Bijenička cesta 46, 10000 Zagreb, Croatia*
[2]*Department of Physics, University of Zagreb, Bijenička cesta 32, 10000 Zagreb, Croatia*
(Dated: May 5, 2014)

We experimentally investigate the radiative force and laser induced fluorescence (LIF) in cold rubidium atoms induced by pulse train (frequency comb) excitation. Three configurations are studied: (i) single pulse train excitation, (ii) two in-phase counterpropagating pulse trains, and (iii) two out-of-phase counterpropagating pulse trains. In all configurations, measured LIF is in agreement with calculations based on the optical Bloch equations. The observed forces in the first two configurations are in qualitative agreement with the model(s) used for calculating mechanical action of a pulse train on atoms, however, this is not the case for the third configuration. Possible resolution of the discrepancy is discussed.

PACS numbers: 32.80.Qk, 37.10.De, 42.50.Nn

I. INTRODUCTION

A train of phase-stabilized femtosecond (fs) pulses in the time domain generates a frequency comb (FC) in the frequency domain (Fig. 1a). The spectrum of the frequency comb consists of a large number of equidistant sharp lines under a smooth envelope. Frequency of an individual FC component,

$$f_N = f_0 + Nf_r,$$

is given by two rf frequencies (the pulse repetition rate f_r and the offset frequency f_0) and the mode number N. By measuring and controlling these two rf frequencies, the frequencies of all FC components can be stabilized with unprecedented accuracy. Frequency comb provides precise frequency markers enabling accurate optical frequency metrology of optical clocks [1–3]. On the other hand, FC represents an ideal tool for atomic and molecular spectroscopy [4, 5]. Considering that FC applications are constantly evolving [6, 7], it is necessary to fully understand the interaction and more specifically the mechanical action of the FC on atomic and molecular systems.

Excitation of an atomic system by the femtosecond pulse train yields coherence effects such as accumulation of the excited state population and atomic coherence, which are consequences of the high phase coherence of the pulses. These effects have been investigated theoretically and experimentally for inhomogeneously broadened alkali vapors in the case of one- and two-photon excitations [8–11]. Constructive and destructive interference was demonstrated for different velocity groups leading to velocity selective excitation of Doppler broadened vapors [12–14].

The coherent effects become more pronounced in atomic systems at low and ultra-low temperatures (no dephasing due to collisions). Somewhat surprisingly, experiments with (ultra)cold atomic gases involving fs pulse trains are scarce in the literature [15–17]. In the pioneer work in Ref. [15], two-photon transitions in cold rubidium atoms were investigated using direct frequency comb

(DFCS) spectroscopy. Coherent pulse accumulation and quantum interference effects were observed. Mechanical action of the frequency comb on the atomic sample due to the first $5S_{1/2}$-$5P_{3/2}$ step of excitation was deduced by monitoring the violet fluorescence from the excited $5D_{5/2}$ state, and modeled by employing the analogy with the continuous wave (CW) radiative force.

A laser cooling scheme using ultrafast pulse trains was proposed for the first time in [18]; it is applicable to atomic species whose level structure makes traditional laser cooling difficult. Doppler cooling with coherent trains of ultrashort laser pulses was investigated in recent theoretical papers [19–21]. Wide spectral coverage of the FC could allow cooling atoms in a broad velocity range simultaneously [21]. Moreover, a FC cooling scheme could enable simultaneous cooling in multiple cooling channels thus enabling simultaneous cooling of multiple atomic species using a single FC source [18, 20]. This holds potential for preparation of coherent ultracold atomic mixtures, which could bring new insights into ultra-cold collisions. However, aside from [15], experimental investigations of the radiative force exerted on atoms by FCs reported in literature are absent, which ultimately provided the motivation for this work.

In this paper we experimentally study laser induced fluorescence (LIF) and radiative force exerted on cold rubidium atoms by fs pulse trains. Two identical pulse trains delayed by τ in the time domain generate a frequency comb with a modulated spectral envelope in the frequency domain. The modulation period, given by $1/\tau$, causes intensity suppression of some FC components, as illustrated in Figs. 1b and 1c. Three configurations are studied: (i) single pulse train excitation [Fig. 1a], (ii) two in-phase counterpropagating pulse trains [Fig. 1b], and (iii) two out-of-phase counterpropagating pulse trains [Fig. 1c]. In configuration (i), there is both transfer of population to the excited state (observed by LIF) and the presence of the radiative force (observed by imaging). In configuration (ii), there is efficient population transfer, but the radiative force on atoms is absent. In the last configuration (iii), we find negligible excited state

population, and no radiative force.

The measured LIF is, in all configurations, in agreement with calculations based on the optical Bloch equations (OBEs). We also study theoretically the radiative force exerted on atoms by a train of pulses by using the model from Refs. [19–21], which takes into account dynamics of the excited state population obtained from OBEs. The model qualitatively explains experiments in configurations (i) and (ii), however, it does not describe experimental results from configuration (iii). Possible resolution of the discrepancy is discussed. In order to model the force, one must connect the internal *quantum* dynamics (obtained from the OBEs) with the motion of the atomic center-of-mass. The latter is *classical* in our MOT system. For the CW laser-atom interaction this connection is well established using the Ehrenfest theorem [22]. However, as we will point out in the discussion following our experiments, the FC can in some geometry and for some parameters probe the boundary between the quantum (internal dynamics) and the classical (center of mass motion) world, which can complicate the calculation of the force induced by the frequency comb.
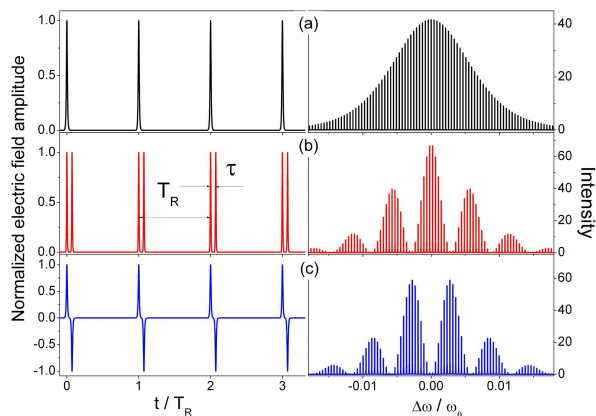

FIG. 1. (Color online) Time and frequency representation of (a) a single fs pulse train [configuration (i)], (b) two identical fs pulse trains delayed by τ [configuration (ii)], and (c) two identical fs pulse trains delayed by τ with π phase differences [configuration (iii)].

II. TWO-LEVEL SYSTEM DYNAMICS DRIVEN BY COUNTERPROPAGATING PULSE TRAINS

In our experiment, the comb parameters are adjusted to drive a single transition $|g\rangle \rightarrow |e\rangle$. Therefore, a model with two-level atoms exposed to fs pulse trains can be used to gain predictions for the experiments. The model is described in detail in our previous work [20]. The internal dynamics of two-level atoms is described by the OBEs using the slowly varying envelope of coherence. The laser field is a sum of the electric fields of the two pulse trains

traveling in the positive and negative x direction, delayed by time τ and phase shifted by $\Delta\varphi$ at $x = 0$. Because the pulse duration τ_p is much smaller than atomic population and coherence relaxation times, and the pulse repetition period T_R, the dynamics is analyzed in four time intervals: interaction (instantaneous) with a pulse traveling in the positive x direction, subsequent atomic relaxation, interaction with a pulse traveling in the negative x direction, and atomic relaxation. These four intervals are repeated with the period T_R. Thus, pulse by pulse temporal evolution of the excited-state population is obtained through the iterative procedure [20].
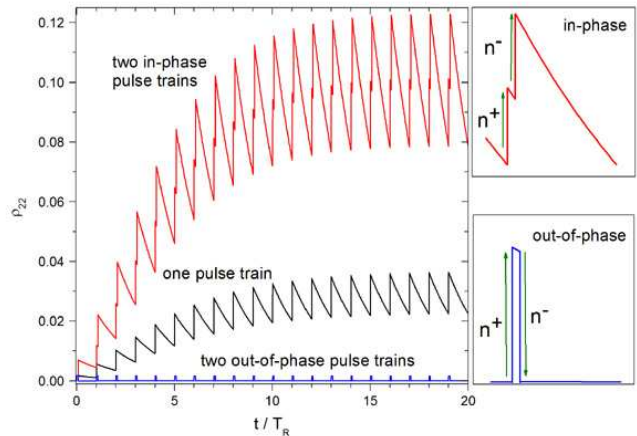

FIG. 2. (Color online) Time evolution of the excited state population (ρ_{22}) of ^{87}Rb-like atoms excited by a single pulse train [black curve; configuration (i)], two in-phase [red curve; configuration (ii)] and two out-of-phase [blue curve; configuration (iii)] counterpropagating pulse trains delayed by $\tau = 0.9$ ns. Inset: zoom-in of one period (T_R) dynamics in the stationary state for two in-phase (red curve) and two out-of-phase (blue curve) counterpropagating pulse trains.

In Fig. 2 we show the time-evolution of the excited state population of two-level atoms (with zero velocity) excited by a single pulse train [black curve; configuration (i)], two in-phase [red curve; configuration (ii)], and two out-of-phase [blue curve; configuration (iii)] counterpropagating pulse trains delayed by $\tau = 0.9$ ns. For the in-phase (out-of-phase) counterpropagating trains, there is zero (π, respectively) phase shift between the trains. The calculations are performed for two-level parameters relevant to the ^{87}Rb D1 resonance at 795 nm (lifetime of 27.6 ns [23]) and fs pulses with $\pi/38$ pulse area.

We see anticipated accumulation of the excited state population for configurations (i) and (ii). In contrast, for the out-of-phase counterpropagating trains [configuration (iii)], there is no accumulation of the excited state population; in the inset we see evidence of the pump-dump dynamics, i.e., the first pulse transfers the population to the excited state which is than depleted by the subsequent out-of-phase pulse. This pump-dump dynamics is repeated with the period T_R. The prediction

of this model for the laser induced fluorescence measurements are clear: we do not expect a LIF signal in the out-of-phase counterpropagating geometry, and the opposite for the in-phase counterpropagating geometry and single train excitation. In order to acquire predictions for the force, one must connect the internal *quantum* dynamics obtained from the OBEs to the center-of-mass dynamics (which is *classical*); this issue is discussed after experiments.

III. EXPERIMENTAL SYSTEM

The experiment was performed using an optical frequency comb emitted from a 100-fs, 80-MHz repetition rate, mode-locked Ti:sapphire laser (Tsunami, Spectra Physics). The peak wavelength of the FC envelope can be tuned within the 740-820 nm spectral range, having a full width at half maximum bandwidth of about 10 nm (5 THz). This corresponds to about 62500 comb modes under the smooth spectral envelope, with a maximum power of 16 μW per comb mode. The frequency comb was not locked externally. The measured frequency drift of a comb mode is about 0.5 MHz for 3.5 minutes acquisition time.

The atomic sample is a cloud of ^{87}Rb atoms trapped and cooled in a glass vapor-cell magneto optical trap (MOT). The trap is set up in the standard σ^+ σ^- retro-reflected configuration, with beam diameters of 2 cm. Cooling and repumper lasers are external cavity diode lasers (ECDL, Toptica DL100 laser systems) delivering total powers of 50 mW and 10 mW, respectively. The cooling laser is typically $2\pi \times 18$ MHz (3Γ) red-detuned from the ^{87}Rb D2 $F_g = 2 \rightarrow F_e = 3$ hyperfine transition. The repumper laser is in resonance with the ^{87}Rb D2 $F_g = 1 \rightarrow F_e = 2$ hyperfine transition, thus keeping most of the population in the $5S_{1/2}$ $F_g = 2$ ground level. The quadrupole magnetic field is provided by a pair of anti-Helmholtz coils, generating a magnetic field gradient of 13 G/cm. The number of atoms in the trap is deduced by measuring the cloud fluorescence with a calibrated photodiode. The cloud density distribution is measured by imaging the cloud fluorescence with a CCD camera, which has a minimal exposure time of 9 μs. Typical CCD exposure time used in the experiments was 220 μs. The observed non-symmetric distribution of atomic density in the MOT is a result of working in the multiple scattering trap regime [24], non-Gaussian intensity distribution of the cooling beams, and the retro-reflected MOT beam configuration. The trap spring constant κ is measured by a transient oscillation method [25]. In typical experimental conditions (13 G/cm - magnetic field gradient, -2.7Γ - cooling laser detuning, 9 mW - total power of the cooling laser before the cell), we obtain a cloud of (0.9 ± 0.1) mm radius that contains about 8×10^8 ^{87}Rb atoms, characterized by a trap spring constant

$$\kappa = (5.3 \pm 0.2) \times 10^{-20} N/m.$$

Spectrally resolved measurements were performed by imaging fluorescence from the cloud onto the slit of a monochromator (Shamrock sr-303i) equipped with a holographic grating (1800 grooves/mm) and a CCD chip based camera (Andor iDus 420). LIF was measured with a 100 μm slit width and 30 ms exposure time and its intensity is proportional to the number of cold atoms in the specific excited state.
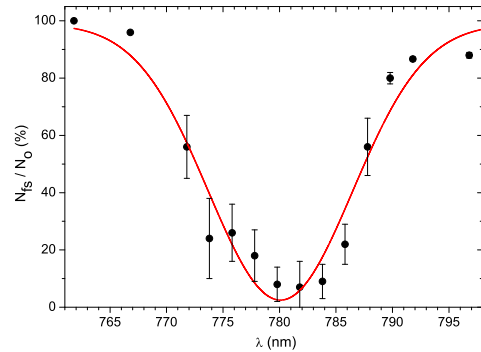

FIG. 3. (Color online) Measured trap loss as a function of the fs laser peak wavelength for the laser power of 700 mW and typical ^{87}Rb MOT parameters.

Resonant action of the fs laser on the cold atomic cloud causes loss of atoms from the MOT, which depends on the fs laser peak wavelength and power. We show in Fig. 3 the measured trap loss as a function of fs laser peak wavelength for a laser power of 700 mW. The number of atoms in the MOT with the fs laser excitation, N_{fs}, is deduced from the LIF measurements and normalized to the number of atoms in the MOT with no fs laser present ($N_0 = 8 \times 10^8$). The maximum trap loss is observed when the fs laser is tuned to the D2 resonance line at 780.2 nm, i.e. when a specific comb line is in resonance with one of the $5S_{1/2} \rightarrow 5P_{3/2}$ hyperfine transitions. Trap loss curve in Fig. 3 reflects the fs laser spectrum of about 10 nm bandwidth, centered at the Rb D2 resonance at 780.2 nm. A similar trap loss curve was observed in [17].

IV. EXPERIMENTAL RESULTS: RADIATIVE FORCE AND LIF

The interaction of cold ^{87}Rb atoms with the frequency comb is studied in three different experimental configurations. In the first configuration, the fs laser beam with a waist of 2 mm is sent directly to the cold cloud (single pulse train configuration, Fig. 1a). Second, the fs laser beam is split with a 50:50 beam-splitter before the MOT cell, and the beams are sent to the cell using the same number of reflections in a counterpropagating arrangement (two in-phase pulse trains, Fig. 1b). In order to increase the beam intensity, the beams are focused with a $f = 500$ mm lens resulting in a beam waist around 250 μm. In the third configuration, the fs laser beam (waist

2 mm) was sent directly on the cold cloud, and then retroreflected by a mirror (two π-out-of-phase counter-propagating pulse trains, Fig. 1c). Time delay between the pulse trains coming from $+x$ and $-x$ directions is adjusted by controlling the optical path length.

To obtain the mechanical force, in every configuration the fs laser wavelength was tuned to 795 nm, corresponding to the ^{87}Rb D1 resonance line, where a smaller transition dipole moment results in smaller trap loss than for the D2 transitions. By manually changing the repetition frequency f_r, one of the comb modes is tuned in resonance with the $5S_{1/2}(F_g = 2) \to 5P_{1/2}(F_e = 1)$ or with the $5S_{1/2}(F_g = 2) \to 5P_{1/2}(F_e = 2)$ hyperfine transition. We have measured LIF at 795 nm which is directly proportional to the $5P_{1/2}$ level population (Fig. 4).
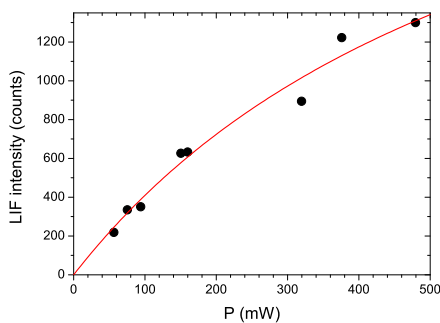

FIG. 4. (Color online) Fluorescence from the cold rubidium cloud induced by the $5S_{1/2}(F_g = 2) \to 5P_{1/2}(F_e = 1, 2)$ excitation using a single frequency comb (points). Data are fitted to a saturation curve (red line).

The radiative force of a single laser beam due to absorption via the D1 resonance is proportional to the excited state population, which saturates at large laser intensities [22], as in Fig. 4. In order to calculate the radiative force, the absolute number of atoms excited by the fs laser to the $5P_{1/2}$ level has to be deduced from the LIF measurements. This is not straightforward and may be subject to experimental error. Moreover, this method is not applicable in the counterpropagating geometry.

For this reason, we use a new approach for measuring the radiative force based on imaging. The fluorescence coming from the cold atom density distribution is imaged by a CCD camera with and without the fs laser excitation. The images are then processed and the displacement Δx from the center of the trap is measured. The radiative frequency comb force is balanced by the MOT trap force $-\kappa \Delta x$, i.e., the radiative comb force is

$$F_r = \kappa \Delta x.$$

We neglect the dissipative part of the cooling force since we are dealing with cold atoms with $v \approx 0$.

A. Single pulse train

Under the action of a single pulse train (the first configuration), the center of mass (CM) of the cloud is displaced by $\Delta x = (0.92 \pm 0.06)$ mm in the direction of the fs laser, see Fig. 6b. This gives $(4.9 \pm 0.4) \times 10^{-23}$ N for the frequency comb force. The total fs laser power of 700 mW results in about 11 μW per comb mode, and 0.35 mW/cm^2 intensity in one comb line.

In order to compare the radiative force due to single spectral line of the frequency comb with the CW radiative force, we have repeated the above procedure using a CW diode laser (instead of the fs laser beam) tuned to the $5S_{1/2}(F_g = 2) \to 5P_{1/2}(F_e=2)$ hyperfine transition. All other experimental parameters were the same as for the single pulse train excitation. The cloud displacement of 0.92 mm was obtained for the CW laser intensity of 0.11 mW/cm^2. These results indicate that the radiative force induced by a single spectral line of the frequency comb is comparable to the CW radiative force.

B. In-phase counterpropagating configuration

The time delay between two counterpropagating pulse trains was set to 0.9 ns by adjusting the optical path lengths of the pulse trains. In Fig. 5 we present the experimental results relevant to the in-phase experimental configuration: the left panel shows cloud fluorescence intensity distribution, while the corresponding LIF spectra are shown on the right panel. The figure displays three experimental arrangements: a) cold cloud (no fs beam), b) cloud excited by a single pulse train coming from the left, and c) cloud excited by two in-phase counterpropagating pulse trains. In the counterpropagating case c), each fs laser beam of 250 mW power is focused to a 250 μm waist on the cloud. In the single beam case b), one of the counterpropagating fs beams from c) is blocked. Although the monochromator resolution is not sufficient to resolve individual hyperfine components, it is straightforward to conclude that LIF at 780.2 nm comes from the $5P_{3/2}(F_e = 3)$ level excited by the cooling laser, whereas LIF at 795 nm comes from the $5P_{1/2}(F_e = 1, 2)$ levels excited by the FC. The population of the excited $5P_{1/2}$ state is much smaller than the population of the $5P_{3/2}$ state (note the different intensity scales of the LIF signals). This is understandable since the cooling transition (D2) is closed with a larger transition dipole moment as opposed to the D1. Additionally, the intensity of the cooling laser is higher than the intensity per comb mode in the FC. LIF at 780.2 nm is proportional to the number of cold atoms in the MOT. The FC radiative force accelerates the atoms; if they are accelerated to velocities larger than the capture velocity, they will escape from the trap and LIF at 780.2 nm will decrease.

From Fig. 5b we see that in the case of single fs beam excitation the CM of the cloud is displaced by (0.28 ± 0.06) mm. Since the fs beams are focused to
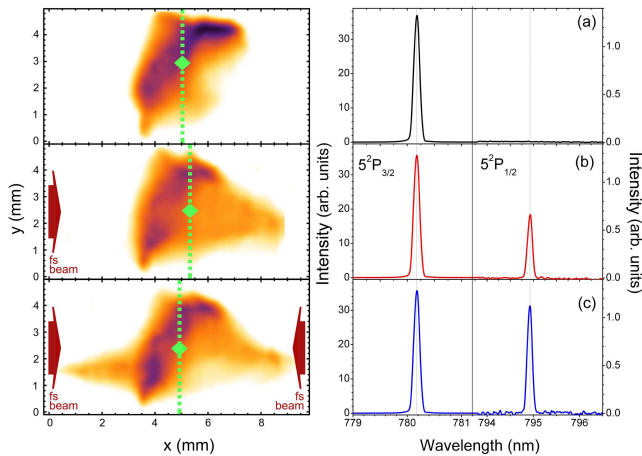
FIG. 5. (Color online) Fluorescence intensity distribution (left panel) and LIF spectra (right panel) of the cold rubidium cloud for: (a) no fs excitation, (b) excited by a single pulse train, and (c) excited by two in-phase counterpropagating pulse trains. Green dashed line indicates the position of the CM of the cloud. Note the different intensity scales of the 780.2 nm and 795 nm LIF signals.

a beam waist which is smaller than the diameter of the cloud (to increase the intensity), the radiative force is non-uniform across the cloud. Thus, the exact force determination method based on the CM displacement is not applicable. However we can see traces of cold atoms pushed out from the trap by the FC force. In the counterpropagating case (Fig. 5c) there is no displacement, i.e., the radiative forces from the two fs beams cancel out. The position of the CM of the cloud is the same as without fs excitation (Fig. 5a) within the experimental uncertainty. LIF at 780.2 nm, which corresponds to the $5P_{3/2}$ excited state population and therefore to the number of atoms in the MOT is also unchanged compared to the case without fs excitation. At the same time, LIF at 795 nm, corresponding to the population in the $5P_{1/2}$ excited state, is about twice as large as in the single pulse train configuration.

C. Out-of-phase configuration

The experimental results for the configuration of excitation by two out-of-phase counterpropagating pulse trains are shown in Fig. 6. The trains were obtained by retroreflecting the incoming pulse train, having beam diameter of 2 mm and total power of 700 mW. Excitation by the incoming (single) pulse train, Fig. 6b, results in the FC radiative force. Cloud CM is displaced by (0.92 ± 0.06) mm. LIF at 780.2 nm decreases almost by a factor of two, suggesting that a significant number of cold atoms is lost from the trap as a result of FC excitation (increased atomic velocities, diffusion and/or optical pumping). In the retroreflected beam configura-
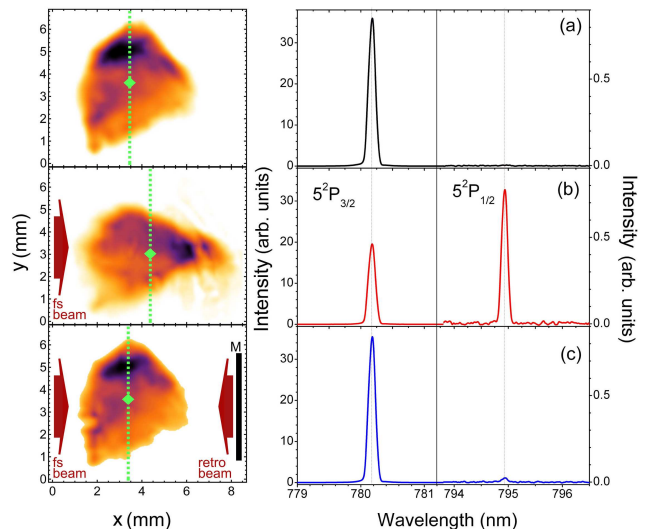

FIG. 6. (Color online) Fluorescence intensity distribution (left panel) and LIF spectra (right panel) of the cold rubidium cloud for: (a) no fs excitation, (b) excited by a single pulse train, and (c) excited by two out-of-phase counterpropagating pulse trains created by retroreflecting the fs laser beam. Green dashed line indicates the position of the CM of the cloud. Note the different intensity scales of the 780.2 nm and 795 nm LIF signals.

tion shown in Fig. 6c, we do not observe the CM displacement within the experimental uncertainty, i.e., we do not observe a mechanical force due to the FC excitation. LIF at 780.2 nm is the same as without the fs excitation, and LIF at 795 nm is practically zero (the residual LIF comes from the imperfect overlap of the two fs laser beams within the cloud). Our experimental results clearly show that no population is transferred to the excited $5P_{1/2}$ state, and no radiative force is induced on the atoms with two out-of-phase counterpropagating pulse trains.

V. DISCUSSION

In this section we discuss and interpret our results, and point out at the possible future directions of research.

A. LIF

The experimental LIF results at 795 nm are in accordance with the solutions of the OBEs plotted in Fig. 2.

In case of single fs laser beam excitation, in Fig. 2 we see that the population of the excited state ($5P_{1/2}$) builds up in time; between pulses the excited state population spontaneously decays to the ground state which corresponds to the LIF measurements presented in Fig. 4.

In case of in-phase counterpropagating pulse trains, in Fig. 2 we also see that the population of the excited state ($5P_{1/2}$) builds up to a larger population as compared to the single pulse train (i.e. when the other is blocked). Again, between the pulses there is spontaneous decay corresponding to the LIF, see Fig. 5c, which is larger than in Fig. 5b when one of the beams is blocked.

In case of out-of-phase counterpropagating pulse trains, in Fig. 2 we see that the population of the excited state does not build up, there is practically no spontaneous decay from the excited state, which corresponds to the fact that LIF is not observed in Fig. 6c.

Based on the experimental results we conclude that the OBEs describe well the internal dynamics of the system.

B. Radiative (mechanical) force

As compared to LIF, the observations of the mechanical force of the fs laser beam(s) are not as simple to explain. The explanation of the mechanical force demands the connection between the internal degrees of freedom (atomic states), and the CM motion (which corresponds to the force). Internal dynamics is quantum and can be successfully explained with OBEs, whereas the CM motion is treated classically. Thus, to understand forces one must make a connection between the (internal) quantum and (CM) classical dynamics. For CW lasers this is made with the use of the Ehrenfest theorem (e.g. see [22]), and two models have been used for pulse trains.

First we discuss the approach used in [15]. Pulse trains create combs in the frequency domain (see Fig. 1). Consider the comb mode which has the frequency closest to the transition frequency $|g\rangle \rightarrow |e\rangle$ (in our experiments this mode is on the D1 resonance). Let us model the interaction as if the laser beam is a CW laser field at that comb mode frequency with the intensity corresponding to that in the comb mode. As we have already discussed above, this simple approach can explain (at least qualitatively) the mechanical action of a single fs laser beam on the cold atomic cloud. Regarding the counterpropagating cases, this approach agrees with the observations because two counterpropagating CW beams at the same frequency form a standing wave which yields zero force in accord with the observations.

However, the use of this naive CW approach should be taken with caution for the following reason. Consider the out-of-phase counterpropagating configuration with π-pulses. In this case, one pulse (from say the left coming pulse train) yields pumping to the excited state of all population that is in the ground state, whereas the next counterpropagating pulse (from the right coming train) yields dumping of all population that is in the excited state. This pump-dump internal dynamics is observed in the solutions of the OBEs. Pumping corresponds to absorption of photons yielding force, but dumping corresponds to stimulated emission of photons yielding force in the same direction because trains propagate in opposite directions. This idea has been used to propose a fs laser induced trapping of atoms in [26, 27] and evidently the CW model should be used with caution, i.e. it is not applicable in every situation.

Next we investigate the model from Refs. [19–21], which can capture the ideas presented in [26, 27]. In the case when the duration of the pulse is much shorter than the repetition time, the pulses provide instantaneous momentum kicks to the atom. The change in momentum of an atom from the n-th pulse $\Delta\mathbf{p}_n$ is given by the difference of the excited state population just after and just before the nth pulse $\Delta\rho_{n,ee}$, and the photon momentum $\hbar\mathbf{k}$ [19–21]:

$$\Delta\mathbf{p}_n = \Delta\rho_{n,ee}\hbar\mathbf{k}. \tag{1}$$

The momentum transfer (averaged over a large number of cycles) due to spontaneous emission is zero, resulting in the total force directed along the laser beam, similar to the CW laser cooling. The radiative force on atoms $\mathbf{F}_r$ is

$$\mathbf{F}_r = \frac{\Delta\mathbf{p}_n + \Delta\mathbf{p}_{n+1}}{\Delta t_{n,n+1}}. \tag{2}$$

Here $\Delta t_{n,n+1}$ is the time-interval corresponding to the two successive kicks; for single pulse train excitation $\Delta t_{n,n+1} = 2T_R$, for counterpropagating configurations $\Delta t_{n,n+1} = T_R$. In the case of single pulse train excitation, in the stationary state $\Delta\rho_{n,ee}$ is equal to 0.0144 (see Fig. 2), yielding the time-averaged radiative force on atoms of about 9×10^{-23} N.

The change of the atomic momentum in the case of excitation by two counterpropagating pulse trains has contributions from pulses in the opposite directions, i.e., the nth pulse will provide a momentum kick $\propto \hbar\mathbf{k}$, the next one $\propto -\hbar\mathbf{k}$, and so on. The constants of proportionality for these two subsequent kicks are given by the changes in the excited state population $\Delta\rho_{n,ee}$ and $\Delta\rho_{n+1,ee}$.

We estimate the force induced by two counterpropagating pulse trains by analyzing the excited state population dynamics in one repetition period T_R, see inset in Fig. 2. In the case of two in-phase pulse trains, the momentum kick from the pulse traveling in the $+x$ direction is equal to the momentum kick from the pulse traveling in the $-x$ direction; $\Delta\rho_{n,ee} \approx \Delta\rho_{n+1,ee}$, i.e., $\Delta\mathbf{p}_n \approx -\Delta\mathbf{p}_{n+1}$, and thus $\mathbf{F}_r \approx 0$, in accordance with observations.

However, in the case of excitation by two out-of-phase counterpropagating pulse trains (see inset in Fig. 2) this model yields the force of 2.1×10^{-23} N, which is only about 4 times smaller than the radiative force exerted on atoms by the single pulse train. This is inconsistent with our observations as we did not observe the radiative force in this case. The force in the model arises due to the pump-dump dynamics, i.e., $\Delta\rho_{n,ee} > 0$ for kicks coming from the left ($\hbar k > 0$), and $\Delta\rho_{n+1,ee} < 0$ for kicks coming from the right ($\hbar k < 0$), yielding $\Delta\mathbf{p}_n \approx \Delta\mathbf{p}_{n+1}$ and $\mathbf{F}_r \approx 2\Delta\mathbf{p}_n/T_R > 0$.

To further investigate this discrepancy, in the right panel of Fig. 7 we show time-evolution of the CM of

the cloud for the cases of no fs excitation (blue triangles), excitation by a single pulse train (black dots), and excitation by two out-of-phase counterpropagating pulse trains (red dots). The single fs train causes the displacement of the cloud CM equal to (0.56 ± 0.05) mm, while in the case of excitation by two out-of-phase counterpropagating pulse trains no cloud CM displacement is measured [Fig. 7 left panel], in contrast with Eq. (2). In addition, we did not observe significant fluctuations of the force around zero in time. For the measurement shown in Fig. 7, we used the fs beam with a diameter of 2 mm, total power of 450 mW, and CCD exposure time of 220 μs.
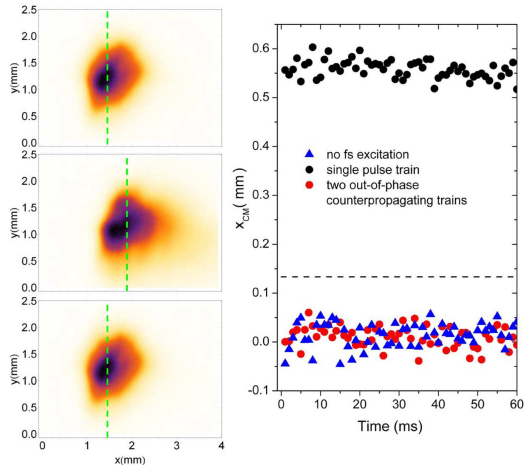

FIG. 7. (Color online) Fluorescence intensity distribution (left panel) and time evolution of the CM coordinate (right panel) of the cold rubidium cloud for the cases of no fs excitation (blue triangles), excitation by a single pulse train (black dots), and excitation by two out-of-phase counterpropagating pulse trains (red dots) created by retroreflecting the fs laser beam. Green dashed line on the left panel indicates the position of the CM of the cloud. Black dashed line on the right panel indicates the expected position of the cloud calculated by using Eq. (2)

.

Here we provide arguments which point out that the discrepancy between the model from Eq. (1) and the experiment can arise because connection between the internal quantum dynamics and classical motion of the CM can be complex for the case of fs laser beams, especially in the out-of-phase counterpropagating geometry where stimulated emission dominates over the spontaneous emission.

The model (1) assumes that after the nth pulse, all the absorbed photons (or photons emitted via stimulated emission) yield the momentum kick $\Delta \mathbf{p}_n = \Delta \rho_{n,ee} \hbar \mathbf{k}$, which changes atom's velocity by $\Delta \mathbf{p}_n / m$. If we treat the CM motion quantum mechanically, the expected value of the momentum transfer during the nth kick is indeed $\Delta \mathbf{p}_n$. However, we may ask what is the quantum mechanical expectation value for the momentum transfer (from the fs beam to the CM motion) after two successive kicks (n and $n+1$)? Is it identical to $\Delta \mathbf{p}_n + \Delta \mathbf{p}_{n+1}$?

The answer to this question is no, and this could be the reason for the discrepancy between our experimental observations and model (1) in the out-of-phase counterpropagating configuration.

In order to clarify this, let us investigate the expectation value for momentum transfer after a single pulse kick, and after two successive pulse kicks (for two counterpropagating out-of-phase pulses). For concreteness, let us assume that the atom is initially in state $|\psi_0\rangle = |g\rangle|K\rangle$, where $|K\rangle$ describes the wavefunction (momentum) of the CM (it could be a wavepacket around momentum K, this would not change the results). Suppose now that a 2θ pulse kicks the atom from the right. The obtained state is

$$|\psi_1\rangle = \cos\theta|g\rangle|K\rangle - i\sin\theta|e\rangle|K+k\rangle,$$

where k is the wavevector of the laser. The expectation value for the momentum transfer is $\sin^2\theta\hbar k$ in accord with model (1).

For simplicity let us neglect spontaneous decay. Let τ be the time that elapsed between the first and the second pulse. The second pulse is a -2θ pulse in the negative direction. It is obvious to see that model (1), which does not account for the entanglement of the internal wavefunction and the CM wavefunction, but only transfers the information on the momentum transfer from the internal dynamics to CM motion, yields $2\sin^2\theta\hbar k$ for the momentum transfer after the two kicks (one $\sin^2\theta\hbar k$ from the pump (2θ), and the other from the dump (-2θ) pulse).

However, if we treat the CM quantum mechanically, after the second kick the atom's wavefunction is

$$\begin{aligned}
|\psi_2\rangle = {} & \cos^2\theta|g\rangle|K\rangle + \sin^2\theta|g\rangle|K+2k\rangle \\
& + i\sin\theta\cos\theta\exp(-i\omega\tau)|e\rangle|K-k\rangle \\
& - i\sin\theta\cos\theta\exp(-i\omega\tau)|e\rangle|K+k\rangle. \quad (3)
\end{aligned}$$

Here, the laser frequency ω, and the transition frequency are identical as we discuss the on-resonance interaction. The expected value for momentum transfer after two kicks is $\sin^4\theta 2\hbar k$, which is much smaller than $2\sin^2\theta\hbar k$ given by model (1); in our experiments $2\theta = \pi/38$ and therefore $\sin^4\theta \ll \sin^2\theta$. Evidently, the force calculated via the expectation value of momentum transfer after two successive kicks can considerably differ from the force calculated via expectation value of momentum transfer after each kick (the expectation value of momentum transfer is divided by the appropriate time interval to obtain the force). Note that since $K \gg k$ (the gas is classical, atoms have velocities on the order of tens of cm/s), $|K+k\rangle \approx |K-k\rangle \approx |K\rangle$ that is $|\psi_2\rangle \approx |g\rangle$ if we separate the CM degrees of freedom from the internal ones (this agrees with the calculation using solely OBEs, i.e., neglecting CM motion which points out that there should not be significant population of the excited state in this case). Note also that for $2\theta = \pi$ pulses, the model (1) works out because all population is transferred in a kick which does not produce entanglement between the internal states and the CM wavefunction.

The CM dynamics, in this system, is classical, and therefore there cannot be entanglement between the CM wavefunction and internal wavefunction for long time-scales. However, our experiments indicate that such an entanglement could survive the time scales longer than two successive counterpropagating fs pulses (0.9 ns). This is an interesting speculation which points out that the mechanical action of fs pulses on cold atoms could in some cases probe the boundary between the quantum and the classical world, and perhaps provide additional knowledge on the processes of decoherence and entanglement.

VI. CONCLUSION

We have investigated the internal dynamics and the radiative force on cold rubidium atoms induced by pulse train (frequency comb) excitation. We found that internal (quantum) dynamics investigated by LIF is well explained by using the OBEs.

Regarding the mechanical action of the fs beam, when a single pulse train is used for excitation, the radiative force is comparable to the CW radiative force (measured under the same experimental conditions), where a comb mode relevant for the excitation can effectively be regarded as a CW laser. This is also evident in the case of excitation with two in-phase counterpropagating pulse trains, where cancelling of the FC radiative forces from the two pulse trains is observed, related to excitation of atoms by both pulse trains (as seen from the LIF spectra). In order to underpin our experiments with theory, we found that the model providing momentum kicks to the atom's CM depending on the internal dynamics [Eq. (1)] is able to explain the mechanical action of the beams in these two configurations.

However, excitation of the atoms by two out-of-phase counterpropagating pulse trains (retro-reflected pulse train) brings an entirely new type of FC-atom interaction. The model providing momentum kicks is not able to describe the experimental findings (i.e. absence of the force) in this particular geometry. The possible explanation of this issue could be that the internal and CM dynamics cannot be treated separately for the short duration of two successive counterpropagating out-of phase pulses. A simple model shows that the generated force depends on how one calculates the quantum mechanical expectation value of momentum transfer, more precisely, after how many pulses is this information transferred to the classical domain.

This discrepancy calls for further theoretical and experimental investigations of the mechanical action of fs beams on cold atoms in versatile geometries. These kinds of experiments hold the potential to provide information on decoherence and entanglement of the inherently quantum states, and states which are in the classical domain. These speculations are underpinned by the fact that LIF which monitors only internal dynamics is well explained by OBEs in all configurations.

Furthermore, the presented results for the out-of-phase pulse train excitation of cold atoms could potentially have an important impact in experiments where the scattered photons are unwanted and the probe laser has to be detuned from the atomic resonance. As a potential application of these results, we foresee nondestructive imaging (PCI) of Bose-Einstein condensates [28] and development of close-to-resonance dipole traps [29].

VII. ACKNOWLEDGMENT

[1] L.-S. Ma, Z. Bi, A. Bartels, L. Robertsson, M. Zucco, R. S. Windeler, G. Wilpers, C. Oates, L. Hollberg, and S. A. Diddams, Science **303**, 1843 (2004).

[2] T. R. Schibli, I. Hartl, D. C. Yost, M. J. Martin, A. Marcinkevičius, M. E. Fermann, and J. Ye, Nature Photon. **2**, 355 (2008).

[3] B. Bloom, T. L. Nicholson, J. R. Williams, S. L. Campbell, M. Bishof, X. Zhang, W. Zhang, S. L. Bromley, and J. Ye, Nature **506**, 71 (2014).

[4] A. Foltynowicz, T. Ban, P. Maslowski, F. Adler, and J. Ye, Phys. Rev. Lett. **107**, 233002 (2011).

[5] P. Maslowski, K. Cossel, A. Foltynowicz, and J. Ye, *Springer Series in Optical Sciences: Cavity-Enhanced Spectroscopy and Sensing: Cavity-Enhanced Direct Frequency Comb Spectroscopy vol. 179* (Springer, Berlin Heidelberg, 2014).

[6] N. R. Newbury, Nature Photon. **5**, 186 (2011).

[7] S. Diddams, J. Opt. Soc. Am. B. **27**, B51 (2010).

[8] D. Felinto, C. A. C. Bosco, L. H. Acioli, and S. S. Vianna, Opt. Commun. **215**, 69 (2003).

[9] D. Felinto, C. A. C. Bosco, L. Acioli, and S. S. Vianna, Phy. Rev. A **64**, 063403 (2001).

[10] A. A. Soares and L. E. E. de Araujo, Phys. Rev. A **80**, 013832 (2009).

[11] D. Aumiler, T. Ban, and G. Pichler, Phy. Rev. A **79**, 063403 (2009).

[12] D. Aumiler, T. Ban, H. Skenderović, and G. Pichler, Phys. Rev. Lett. **95**, 233001 (2005).

[13] T. Ban, D. Aumiler, H. Skenderović, and G. Pichler, Phys. Rev. A **73**, 043407 (2006).

[14] N. Vujičić, T. Ban, G. Kregar, D. Aumiler, and G. Pichler, Phy. Rev. A **87**, 013438 (2013).

[15] A. Marian, M. C. Stowe, J. R. Lawall, D. Felinto, and J. Ye, Science **306**, 2063 (2004).

[16] A. Marian, M. C. Stowe, D. Felinto, and J. Ye, Phys. Rev. Lett. **95**, 023001 (2005).

[17] A. V. Akimov, E. O. Tereshchenko, S. A. Snigirev, and A. Y. Samokotin, Journal of Experimental and Theoretical Physics **109**, 359 (2009).

[18] D. Kielpinski, Phys. Rev. A **73**, 063407 (2006).

[19] E. Ilinova, M. Ahmad, and A. Derevianko, Phys. Rev. A **84**, 033421 (2011).

[20] D. Aumiler and T. Ban, Phys. Rev. A **85**, 063412 (2012).

[21] E. Ilinova and A. Derevianko, Phys. Rev. A **86**, 023417 (2012).

[22] H. J. Metcalf and P. van der Straten, *Laser Cooling and Trapping* (Springer-Verlag, New York, 1999).

[23] D. A. Steck, *Quantum and Atom Optics* (available online, `http://steck.us/teaching`, 2007).

[24] C. G. Townsend, N. H. Edwards, C. J. Cooper, K. P. Zetie, and C. J. Foot, Phys. Rev. A **52**, 1423 (1995).

[25] K. Kim, K.-H. Lee, M. Heo, H.-R. Noh, and W. Jhe, Phys. Rev. A **71**, 053406 (2005).

[26] T. F. I, J. Walz, and T. Hansch, Optics Communications **117**, 262 (1995).

[27] V. Romanenko and L. Yatsenko, J. Phys. B: At. Mol. Opt. Phys. **44**, 115305 (2011).

[28] R. Meppelink, R. A. Rozendaal, S. B. Koller, and P. van der Straten, Phys. Rev. A **81**, 053632 (2010).

[29] R. Grimm, M. Weidemüller, and Y. Ovchinnikov, Adv. At. Mol. Opt. Phys. **42**, 95 (2000).